KODAIKANAL OBSERVATORY
BULLETIN Number 186

Line Profile Analysis of Carbon Molecules in the Sun

Nirupama Raghavan*

Abstract

Thirteen molecular lines of CN, C_2 and CH have been photoelectrically observed at six disc positions each. The observed trends fall into two categories; one for strong lines and another for weak lines, irrespective of the molecule of their origin. Detailed profile calculations have been made for six selected lines. LTE methodology and an anisotropic model of turbulence have been assumed. In the region of line formation for these molecules (τ=0.1 to 0.04) ξ_{rad} and ξ_{tan} are 3.0 km/sec and 3.6 km/sec respectively. An interesting variation of the factor F, used for fitting central intensities with μ is found. It is strongly suspected that important physical reasons underlie this variation.

Ever since Peckers group (1949, 1950, 1952) studied the centre-limb variation of equivalent widths of resolved and unresolved CN, CH and C_2 lines, the problem of correctly interpreting these variations has remained. Calculations based both on pure scattering and pure absorption mechanisms of line formation have predicted equivalent widths that are larger than the observed ones at the limb.

The following ideas have been put forward to remove the discrepancy:

(a) Existence of non-LTE effects as are present in the formation of atomic lines (Pecker and Praderie 1960).

and (b) Presence of unsuspected polyatomic molecules involving carbon (Laborde 1961).

Although these have changed the equivalent widths in the right direction, the agreement has not been improved significantly.

This problem has been heightend by more recent observations by Newkirk (1957) Laborde (1961) and Cowley (1964). Newkirk's analysis of excellent observations of CO lines has shown that the Aller-Pierce model along with the mechanism of pure absorption explains the C-L observations very satisfactorily. Using Minnaert's photospheric model, Laborde predicts the C-L variation of MgH lines correctly, while for C_2 the observed and predicted variations are very different. Cowley's results for CN proves that LTE calculation of equivalent width is entirely adequate for the centre of the disc observations. We are led to conclude, therefore, that:

(i) A conventional model of the photosphere is adequate for both a molecule like MgH formed relatively lower in the atmosphere ($\bar{\tau}_o$ (MgH) > 0.1) and a molecule like CO formed higher up ($\bar{\tau}_o$ (CO) $\leqslant .01$)

*Now at the Department of Physics, Indian Institute of Technology, Kanpur.

(ii) Calculations based on a similar frame work are also correct at $\mu=1.0$ for molecules like CN ($\bar{\tau}_0$ (CN)$\leq$0.06

(iii) It has *not* been possible to predict the C-L variations of CN, CH and C_2 on the basis of LTE methodology, coupled with conventional models.

It is evident that the cause for the discrepancy lies in a direction that has not yet been explored and a re-examination of the problem is necessary. The crucial question is, why is LTE methodology inadequate for all observed carbon constituent molecules except CO? In fact CO being formed in the highest layers, should be affected more by deviations from LTE. Also is $T_{exc} \neq T_a$ the only way in which non LTE effects enter the molecular problem? These are the questions that must be looked into.

Another aspect of interest regarding carbon molecules, arises from the fact that they exist in a narrow layer in the transition region between the photosphere and the chromosphere. This enables one to use these molecules for studying the structure of this region; especially of interest is the determination of turbulence velocity as can be appreciated from Fig. 1. In the hatched region there are no velocity determinations and it is

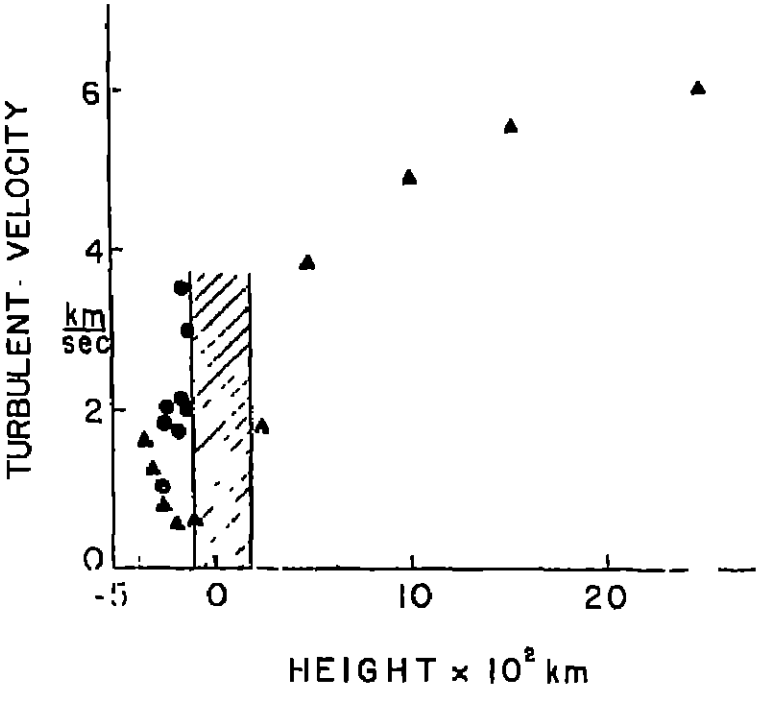

Fig 1. The known variation of turbulent velocities with height in the solar atmosphere. The shaded area is the region of interest in this investigation; triangles represent Unno's results and circles the results of other workers.

precisely here that the molecules are formed. In his fine analysis of CN lines, Cowley states that his results are insensitive to both the model of turbulence and its magnitude. While this may be true for equivalent widths, profile shapes are sensitive to both.

The object of this investigation has, therefore been:

(1) to study differentially, C-L variation of line profiles of the Carbon molecule CN, CH and C_2

(2) to derive turbulence velocity from these profiles, on the basis of LTE methodology.

OBSERVATIONS

The solar tower telescope of 38cm aperture of the Kodaikanal Observatory has been used in this work. This gives a 34 cm image (scale 5″ arc/mm). The image it guided by an electro-mechanical system, with respect to a pattern of circles drawn as specific μ values, and mounted at the plane of the focussed image.

The 18.3 meter Littrow spectrograph has a 200 × 135 mm Babcock grating. The 4th, 5th and 6th orders were used in this study. The dispersion in the 5th order at 5000Å is 10 mm/Å.

The profiles were traced photoelectrically. The scanner had a speed of 3mm/minute so that scanning rate of 5mÅ/sec is achieved. At the dispersion used the scanning slit isolated 3mÅ of the spectrum. The output was amplified by a D. C. amplifier and fed to a Brown recorder with a $\frac{1}{8}$ sec time constant. The sky transparency was monitored by a stationary photomultiplier tube, centred on the nearby continuum.

Instrumental Profile

The instrumental profile was derived by tracing an iodine absorption line at 5318.610Å in the 5th order. A 10 cm column of iodine vapour was placed in the Solar beam just ahead of the slit. The pressure of Iodine was controlled by visually examining whether very close doublets at ($\Delta\lambda \leq 10$mA) at 5330.10 , 5330.33 and 5333.57Å were well resolved. The half width of the instrumental profile with a 2.4 normal slit was 13mA.

The observed profiles were corrected for finite resolving power by the graphical method suggested by Bracewell (1955), which is quick and of useful accuracy. The maximum correction to the central intensity for resolving power was 0.8% of the continuum intensity.

Scattered Light

If 'g' gives the excess scattered light, the true relative intensity at any point on the profile is given by

$$I_{true} = (I_{obs} - g)/(I_{continuous} - g)$$

Diffuse scattered light was taken into account by registering the signal with the ruled area of the grating masked and the scanning slit centred on the continuum. This signal was used as the reference dark level, over which all measurements were made.

To correct for Rowland ghosts, g is obtained from the above equation by combining the observed central intensities of H_γ, Mg b_1 and Na D_1 and D_2 in the 6th, 5th and 4th orders with the Sacramento Peak double pass observations of the same lines (White 1962, Waddell 1962 and 1963). To check the accuracy of this method, 'g' was evaluated from the central intensity of Mgb_1 and the other parts of the line were corrected using this 'g'. Double pass and the corrected single pass profiles, coincided with each other, over the entire profile, within one percent.

Table I sets out the details of observations. The profiles were measured in all cases with respect to the local continuum which is the same as the general continuum given by the Utrecht Atlas except for CN lines at 3864Å and 3879Å. Profile measurements for these two lines were referred to an arbitrary continuum which matched the general continuum of Utrecht atlas. This amounted to changing the residual intensities referred to the local continuum by a factor of 0.95.

TABLE I

Details of the Photoelectric observations included in this study

Date of Observation	Wavelength	Molecule	Transition	Rowland Intensity	Seeing	Transmission	Location of local continuum
1 April 1964	3864.807Å	CN	$^2\Sigma - ^2\Sigma$	3	>2 Average	V. Fair	3863.25
2 April 1964	3879.578Å	CN	$^2\Sigma \quad \Sigma^2$	1	2 to 3	Good	3880.55
	3879.661Å			0			
	3879.716Å			0			
30 March 1964	4192.917Å	CN	$^2\Sigma - ^2\Sigma$	−1	2 to 3	V. Fair	4192.80
11 March 1964	4207.409Å		$^2\Sigma - ^2\Sigma$	1	2 to 3	Good	4207.65
14 March 1964	4212.236Å	CN	$^2\Pi_u - ^2\Pi_g$	−1	about 2	Fair	4212.50
	4212.407Å			−1			
18 March 1964	5086.251Å	C_2	$^3\Pi_u - ^3\Pi_g$	−1	about 2	V. Fair	5086.15
	5086.399Å			−2			
17 March 1964	5094.029Å	C_2	$^3\Pi_u - ^3\Pi_g$	−2	< 3	Good	5093.90
24 March 1964	5147.106Å	C_2	$^3\Pi_u - ^3\Pi_g$	2 — 2	2 to 3	Good	5145.95
26 March 1964	5159.467Å	C_2	$^3\Pi_u - ^3\Pi_g$	−3	2 to 3	Fair	5158.25
	5159.609Å						
14 March 1964	4210.970Å	CH	$^2\Delta - ^2\Pi$	−3	2 to 3	Fair	4212.50
15 March 1964	4218.726Å	CH	$^2\Delta - ^2\Pi$	−3	> 2	V. Fair	4218.60
16 March 1964	4281.974Å	CH	$^2\Delta - ^2\Pi$	−2	> 2	V. Fair	4281.65
28 March 1964	4378.915Å	CH	$^2\Delta - ^2\Pi$	−2	2 to 3	Good	4378.75

Pencilled copies of the profile on transparent graph sheets were obtained and measured at every millimeter, dispersion on the traces ranging from .007Å/mm to .005Å/mm. The average of atleast six such traces was plotted to a large working scale and corrected for instrumental profile and scattered light.

Description of the observed profiles

3864.307Å CN: This is a close spin doublet with a separation of less than 15mA and rotational quantum number K=14. The central intensity increases from centre to limb, slowly at first and steeply later. The half width also increases towards the limb, so that the equivalent width remains nearly constant. The profile takes a characteristic U—shape towards the limb.

3879.579Å
3879.661Å } CN is a triplet of the 0—0 vibrational transition; K=9, 48
3879.716Å and 48 respectively.

Towards the limb, the profiles become shallow and broad keeping the total absorption due to the three lines effectively constant.

4192·917Å CN comprises of three lines of 4192, 898Å. 4192.898Å and 4192.962 of the 0—1 vibrational transition.

The latter two have K=40 of the P branch and the former K=0 of the R branch. The profile has a pronounced red asymmetry, as is to be expected in view of the presence of the 4192.962Å line. Central intensity decreases in going towards the limb. The half widths, however, increase and the profile becomes U shaped towards the limb.

4207.409Å line of CN is a doublet of 4207.399 and 4207.468Å. Central intensity rises steeply with decreasing μ. At the limb, the profiles are U shaped, broader and shallower.

4212.215Å, 4212.275Å and 4212.399Å are CN lines with $\Delta V = -1$. The first two are spin doublets with K=38 and 4212.399Å has K=7. The C-L decrease of the central intensity of the unresolved spin doublet is more rapid than that of 4212.399Å.

4210.970Å of CH has K=16 and is a doublet of R_{2ed} and R_{1ed} components. The line has a violet asymmetry. Like the strong lines of CN, r_0, the central intensity increases towards the limb and the profile is once again U shaped at the limb. 4218.726Å of CH is a doublet comprising of the R_{1de} and the R_{2de} components of K=15. This has a slight red asymmetry and has the same characteristic C-L variation of central intensity and half width as the 4210Å line of CH.

4281.974Å of CH also behaves similarly on going from centre to limb. This line comprises of the $Q_{1d}+Q_{2d}$ components of K=22.

4378.915Å of CH is in the P branch of 1—1 vibrational transition with K=15 and is made up of the P_{1de} and the P_{2de} components. The line has a C-L variation of r_0 and half width similar to the weaker lines of CN, *i.e.*, 4192 and 4212Å

5086.251Å, 5086.399Å are partially resolved C_2 triplet of the Swan system. 5086.251 is the unresolved $R_{23}(37)$ line and 5086.399Å, the $R_1(37)$ line. The lines are broader and deeper towards the limb, following the pattern of the weak lines of CN. 5094.029 of C_2 comprises of the unresolved $P_{21}(62)$ at 5094.002 and $P_1(62)$ at 5094.025.

This weak line has a central intensity of 91.7% at the centre, which decreases to 90.6% at $\mu=0.25$. Again the half width increases towards the limb and the profile becomes markedly U shaped on going from $\mu=0.35$ to $\mu=0.25$. 5147.106A of C_2 is a $R_1(11)$ line and is blended on both wings. The slight violet asymmetry may be an atomic blend effect. Neither the central intensity nor the half width increase very much until $\mu=0.35$. From $\mu=0.35$ to $\mu=0.25$ the increase in r_c and half width is relatively more marked.

5159.467A and 5759.609A of C_2 are $P_{21}(28)$ and $P_1(28)$ lines of the Swan system. Their C-L variation follows the same pattern set by other weak lines of CN and C_2 described above.

The observed profiles are given in numerical form in Table II. Fig 2, gives the observed C-L variation of central intensities r_c for strong and weak lines. Summarising the general trends, we find that lines are broader at the limb than at the centre in all cases. r_c shows a decrease up to $\mu=0.45$ and then increases slowly for weak lines. For all strong lines irrespective of the parent molecule, r_c increases slowly up to $\mu=0.7$ and then increases more steeply.

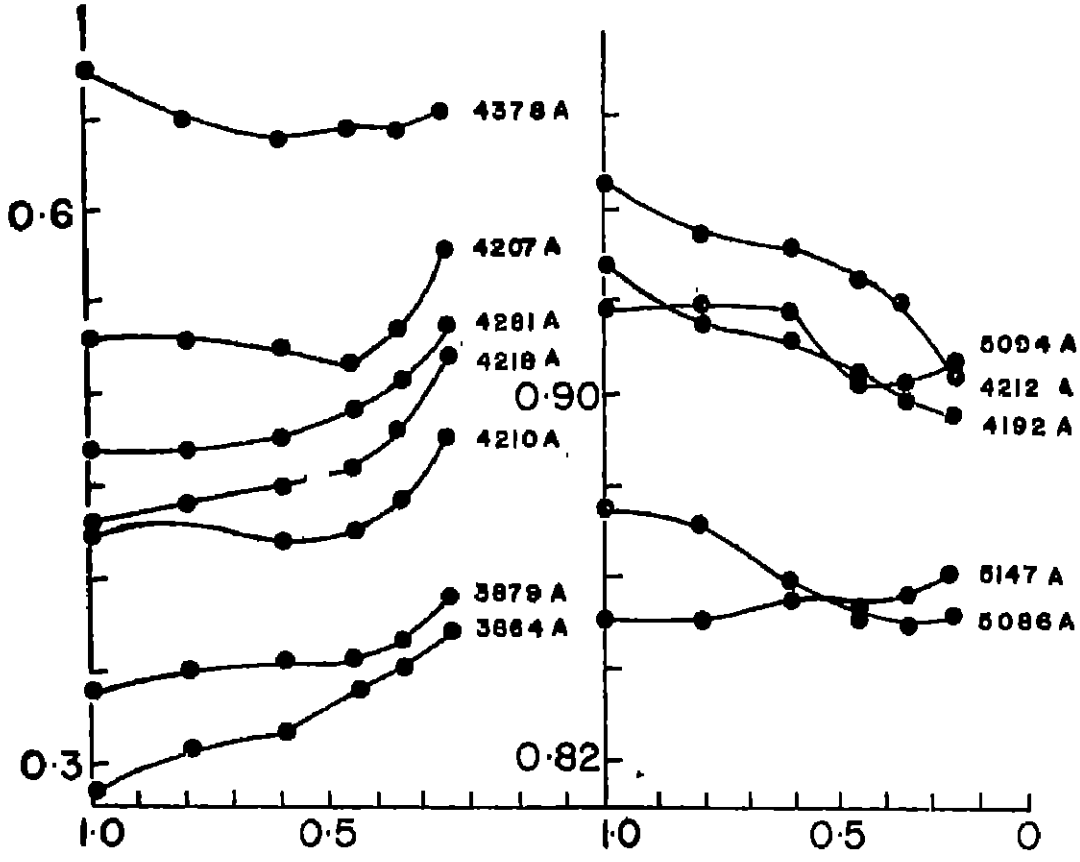

Fig. 2. Observed variation of central intensities for strong and weak lines.

The generality of the trends indicates that the C-L variations are characteristic of the physical structure of the solar atmosphere rather than a property of the particular molecule concerned. Some factor affecting all three molecules identically could, however, be the reason for the similarity in the C-L variation.

TABLE II

Δλin mA	μ = 1.00		μ = 0.80		μ = 0.60		μ = 0.45		μ = 0.35		μ = 0.25	
	Violet	Red	Violet	Red	Violet	Red	Violet	Red	Violet	Red	Violet	Red
					3864.307Å *CN							
0	0.295	0.295	0.310	0.310	0.315	0.315	0.340	0.340	0.350	0.350	0 370	0·370
20	0.355	0.355	0.355	0.355	0.395	0.385	0.387	0.380	0.390	0 385	0.405	0 405
40	0.560	0.560	0.525	0.520	0.555	0.530	0.545	0.535	0.530	0.525	0 535	0·535
60	0.778	0.768	0.730	0.695	0.730	0.695	0.700	0.710	0.695	0.690	0.710	0.700
80	0.825	0.815	0.810	0.810	0.815	0.800	0.807	0.805	0.815	0.800	0.780	0.762
100	0.835	0.825	0.820	0.825	0.835	0.820	0.830	0.825	0.830	0.820	0.812	0.810
120											0.820	0.820
					4192.917 Å* CN							
0	0.926	0.926	0.915	0.915	0.911	0.911	0.903	0.909	0.898	0.898	0.894	0.894
20	0.988	0.933	0.928	0.924	0.919	0.921	0 912	0.912	0.902	0.902	0.904	0.903
40	0.966	0.948	0.957	0.939	0.940	0.941	0.941	0.934	0.925	0.993	0.924	0.924
60	0.987	0.963	0.984	0.956	0.963	0.962	0.966	0.955	0.961	0.958	0.962	0.950
80	0.996	0.979	0.998	0.975	0.984	0.985	0.985	0.978	0.994	0,977	0.987	0 978
100	1.000	0.990	0.998	0.993	0.994	0.997	0.996	0.991	0.998	0.994	0 997	0.996
120	1.000	0.998	1.000	1.000	1.000	0.999	1.000	0.998	1.000	1.000	1.000	1.000
140		1.000			1.000	1.000		1.000				
					4207.409° A*CN							
0	0.590	0.580	0.580	0.590	0.525	0.525	0.515	0.515	0.595	0.595	0.580	0.580
20	0.560	0.555	0.570	0.565	0.540	0.545	0.540	0.545	0.550	0.560	0 598	0.598
40	0.640	0.640	0.642	0.625	0.620	0.615	0.595	0.620	0.605	0.620	0.660	0.655
60	0.750	0.750	0.750	0.740	0.730	0.728	0.695	0.710	0.700	0.700	0.755	0.735
80	0.855	0.845	0.857	0.845	0.825	0.815	0.792	0.800	0.790	0.810	0.860	0.830
100	0.982	0.900	0.926	0.900	0.900	0.890	0.870	0.870	0.882	0.875	0.913	0.890
120	0.955	0.940	0.955	0.937	0.940	0.925	0.920	0.913	0.920	0.920	0.955	0.937
140	0.950	0.960	0.960	0.962	0.955	0.945	0.990	0.940	0.917	0.950	0.965	0.960
160		0.970	0.940	0.980	0.950	0.960	0.925	0.950	0.910	0.965	0.935	0.975
180		0.975		0.980		0.965		0.960		0.975		0.980

*Refers to the wavelength of the centre of the line as given in the Revised Rowland Table.

TABLE II—*Contd.*

$\Delta\lambda$ in mÅ	$\mu = 1.00$ Violet	$\mu = 1.00$ Red	$\mu = 0.80$ Violet	$\mu = 0.80$ Red	$\mu = 0.60$ Violet	$\mu = 0.60$ Red	$\mu = 0.45$ Violet	$\mu = 0.45$ Red	$\mu = 0.35$ Violet	$\mu = 0.35$ Red	$\mu = 0.25$ Violet	$\mu = 0.25$ Red
					5094.029Å * C_3							
0	0.917	0.917	0.918	0.918	0.918	0.918	0.901	0.901	0.901	0.901	0 906	0.906
20	0.927	0.926	0.929	0.925	0.931	0.925	0.912	0.910	0.919	0.914	0.914	0.913
40	0.942	0.938	0.931	0.935	0.947	0.937	0 932	0.924	0.936	0.927	0.932	0.924
60	0.963	0.951	0.955	0.947	0.964	0.948	0.953	0.935	0.957	0.939	0.953	0.937
80	0.978	0.962	0.975	0.957	0.981	0.959	0.971	0.945	0.974	0.950	0.969	0.949
100	0.992	0.973	0.991	0.967	0.993	0.969	0.985	0 957	0.988	0.960	0.983	0.961
120	0.997	0.982	0.998	0.975	0.999	0.976	0.994	0.968	0.994	0 969	0.992	0.971
140	0.999	0.989	0.999	0.982	1.000	0.984	0.999	0.978	0.999	0.976	0.997	0.979
160	1.000	0.994	1.000	0.988		0.990	1.000	0.986	1.000	0.983	1.000	0.985
180		0.997		0.993		0.995		0.992		0.988		0.990
200		0.999		0.996		0·998		0.997		0.993		0.994
220		1.000		0.999		1.000		1 000		0.996		0.997
240				1.000						0.999		0.999
					5147.106A* C_2							
0	0.850	0.850	0.851	0.851	0.856	0.856	0.851	0.851	0.854	0.854	0 860	0.860
20	0.862	0.862	0.859	0.862	0.870	0.870	0.865	0 864	0.870	0.869	0.869	0 869
40	0.890	0.888	0.884	0.890	0.897	0.903	0.890	0.894	0.891	0.890	0.890	0.897
60	0.920	0.932	0.913	0.926	0.928	0.938	0.918	0 924	0.924	0.918	0.916	0.924
80	0.946	0.959	0.937	0.948	0.958	0.962	0.942	0.947	0.948	0.944	0.940	0.947
100	0.962	0.964	0.952	0.964	0.965	0.974	0.956	0 963	0.952	0.960	0.959	0.965
120	0.971	0.973	0.962	0.974	0.973	0.978	0.965	0.973	0.960	0.969	0 963	0.975
140	0.974	0.976	0.971	0.978	0.976	0.982	0.968	0.979	0.962	0.977	0.961	0.981
160	0.969	0.980	0.974	0.980	0.970	0.980	0.965	0.980	0 956	0.981	0.958	0.982

*Refers to the wavelength of the centre of the line as given in the Revised Rowland Table.

TABLE II—*Contd.*

$\Delta\lambda$ in mÅ	$\mu = 1.00$ Violet	Red	$\mu = 0.80$ Violet	Red	$\mu = 0.60$ Violet	Red	$\mu = 0.45$ Violet	Red	$\mu = 0.35$ Violet	Red	$\mu = 0.25$ Violet	Red
					4210.970Å* CH							
0	0.425	0.425	0.430	0.430	0.420	0.420	0.430	0.430	0.442	0.442	0.485	0.485
20	0.440	0.445	0.450	0.417	0.435	0.437	0.442	0.447	0.460	0.460	0.497	0.495
40	0.500	0.535	0.515	0.535	0.495	0.460	0.472	0.485	0.477	0.487	0.537	0.530
60	0.595	0.670	0.595	0.645	0.575	0.609	0.555	0.595	0.565	0.605	0.610	0.605
80	0.700	0.795	0.715	0.760	0.680	0.723	0.635	0.735	0.650	0.705	0.692	0 708
100	0.785	0.865	0.793	0.855	0.705	0.810	0.765	0.825	0.740	0.807	0.775	0.798
120	0.855	0 895	0.875	0.905	0.840	0.875	0.842	0.875	0.825	0.862	0.840	0.868
140	0.917	0.910	0.925	0.920	0.897	0.907	0.887	0.900	0.885	0.895	0.890	0·907
160	0.937	0.915	0.935	0.925	0.922	0.925	0.925	0.915	0.923	0 907	0.925	0.920
180	0.950	0.930	0.945	0.925	0.925	0.927	0.940	0.910	0.923	0.910	0 925	0.920
200			0.950									
					4218.726Å* CH							
0	0.430	0.430	0.440	0.440	0.450	0.450	0.460	0.460	0.480	0·480	0.517	0.517
20	0.462	0.458	0.478	0.473	0.478	0.475	0.490	0 405	0.300	0.505	0.535	0·538
40	0.575	0.565	0.570	0.568	0.585	0.580	0·582	0.570	0.565	0 581	0·597	0.600
60	0.735	0.730	0.730	0.710	0.715	0.710	0.710	0.690	0.695	0.700	0.700	0·717
80	0.870	0.875	0.870	0.830	0.832	0.845	0.830	0·812	0.820	0.815	0.810	0.850
100	0 945	0 930	0.955	0.955	0.955	0.925	0.930	0.890	0.915	0.895	0.915	0 917
120	0.992	0.948	0 990	0.975	0 978	0 960	0.965	0 940	0 960	0.940	0 970	0.950
140	0·997	0·972	0.998	0·985	0.992	0.978	0.982	0.965	0 997	0.962	0.987	0.967
160	1·000	0·975	1·000	0·985	1·000	0.982	0.992	0.972	1.000	0.970	0.997	0.972
180							1 000				1.000	

*Refers to wavelength of the centre of the line as given in the Revised Rowland Table.

TABLE II—*Contd.*

$\Delta\lambda$ in mÅ	$\mu = 1.00$ Violet	Red	$\mu = 0.80$ Violet	Red	$\mu = 0.60$ Violet	Red	$\mu = 0.45$ Violet	Red	$\mu = 0.35$ Violet	Red	$\mu = 0.25$ Violet	Red
					4281.974Å* CH							
0	0.467	0.467	0.470	0.470	0.475	0.475	0.490	0.490	0.505	0.505	0.533	0.535
20	0.490	0.495	0.497	0.500	0.490	0.495	0.507	0.512	0.522	0.525	0.550	0.560
40	0.565	0.560	0.565	0.570	0.555	0.557	0.565	0.570	0.580	0.570	0.595	0 600
60	0.697	0.690	0.680	0.680	0.665	0.660	0.650	0.665	0.665	0.665	0.670	0 685
80	0.822	0.820	0.795	0.800	0.790	0.780	0.780	0.810	0.810	0.751	0 770	0.770
100	0.908	0.895	0.915	0.880	0.895	0.860	0.890	0.862	0.895	0.845	0·865	0.855
120	0.965	0.930	0.965	0.915	0.950	0.910	0.950	0.920	0.945	0.902	0.930	0.900
140	0.982	0.945	0.990	0.930	0·977	0.930	0.975	0.935	0.975	0.930	0 960	0 930
160	0.997	0.915	1.000	0.945	0.992	0.935	0 990	0.995	0 990	0.995	0 985	0 930
180	1.000	0.915	1.000	0·945	1.000	0.935	1.000	0.985	0.995	0.995	0 995	0 915
200									1·000		1.000	
					4378 915Å* CH							
0	0.675	0.675	0.650	0.650	0.640	0.640	0.645	0.645	0.640	0.640	0.655	0.655
20	0.700	0.702	0.680	0.680	0.665	0.665	0.670	0.667	0.665	0.658	0 675	0.670
40	0.780	0.752	0.752	0.727	0.740	0.710	0.740	0·712	0.725	0.698	0.732	0.710
60	0.870	0.805	0.850	0.780	0.835	0.760	0.832	0.757	0.805	0.752	0.818	0.755
80	0.950	0.855	0.915	0.832	0.955	0.810	0.990	0.807	0.898	0.802	0 895	0.807
100	0 980	0.890	0.962	0.872	0.980	0.855	0.907	0.850	0.942	0.842	0.943	0.845
120	0.995	0.905	0.975	0.898	0.992	0.878	0 983	0.880	0.970	0.865	0.975	0 870
140	1.000	0.915	0.989	0.915	0.997	0.890	0.992	0.898	0.980	0.882	0 990	0 888
160		0.930	0.992	0.922	1.000	0.902	1.000	0.912	0 992	0.895	0 997	0.900
180			1.000						1.000		1.000	

*Refers to the wavelength of the centre of the line as given in the Revised Rowland Table.

TABLE II—*Contd.*

Δλ in mÅ	μ=1·00	μ=0·80	μ=0·60	μ=0·45	μ=0·35	μ=0·25
			3879·118Å* CN			
0	0.843	0.817	0.835	0.840	0.817	0·823
20	0.815	0 845	0.835	0.847	0.040	0·042
10	0.842	0.847	0.835	0.810	0.840	0.837
60	0.892	0.890	0.020	0.817	0.825	0·812
80	0.810	0.805	0.760	0.760	0.762	0·740
100	0.720	0.730	0.675	0.645	0 660	0 620
120	0.575	0.515	0.515	0.485	0.525	0 495
140	0.400	0.390	0.395	0.395	0.405	0 410
160	0.335	0.350	0.360	0.360	0.365	0·390
180	0·420	0·390	0·390	0·375	0.390	0.410
200	0·475	0·432	0·410	0·395	0·402	0.412
220	0·395	0.390	0.370	0.360	0.370	0.387
240	0.355	0.350	0·355	0·348	0.355	0.382
260	0.390	0.365	0·955	0·350	0·302	0 390
280	0.375	0·360	0.372	0·372	0.380	0.405
300	0·385	0·385	0.420	0·425	0.420	0 455
320	0.515	0.490	0·570	0.595	0·560	0 595
34	0·790	0·690	0·720	0·720	0·600	0.725
360	0.850	0.790	0.805	0.800	0·795	0.810
380	0·850	0.812	0·845	0·812	0.820	0·815
400		0·760	0·760	0·810		
			4212·116Å * CN			
0	0·980	0·989	0.902	0.982	0.979	0.976
20	0.892	0.985	0.985	0.984	0·977	0.977
40	0·989	0·977	0·981	0·974	0·904	0·972
60	0·976	0·962	0·902	0·957	0·918	0·931
80	0·950	0·949	0·946	0·948	0·932	0·928
100	0·949	0 930	0·935	0·919	0·922	0·911
120	0·914	0·934	0·951	0·923	0·919	0·904
140	0·951	0·940	0·935	0·929	0·924	0·910
160	0.901	0·932	0·918	0·912	0·936	0 925
180	0·972	0·966	0·962	0·902	0·933	0·958
200	0·962	0·979	0·977	0·989	0·900	0·978
220	0·988	0·986	0·983	0·996	0·983	0.983
240	0·981	0·970	0·973	0·977	0·969	0·968
260	0·909	0·952	0·957	0·957	0·917	0·951
280	0·950	0·951	0·949	0·947	0·938	0·938
300	0·961	0·970	0·904	0·963	0·953	0·952
320	0·980	0.994	0·978	0·979	0·975	0·978
340	0·993	0·995	0·994	0·992	0·992	0·991
360	0·998	1·000	1·000	1·000	0·998	1·000
380	1·000				1·000	

*Indicates that residual intensities have been measured from this position, in steps of 20mÅ towards the long wavelength.

TABLE II—*Contd.*

Δλin mÅ	μ=1.00	μ=0.80	μ=0.60	μ=0.15	μ=0.35	μ=0.25
			3083.071Å* C_4			
0	1.000	0.998	0.998	0.998	1.000	1.000
20	1.000	1.000	1.000	1.000	0.998	0.998
40	0 999	0.996	0.998	0.998	0 994	0.992
60	0.999	0.991	0.991	0.993	0.989	0.980
80	0.984	0.982	0.976	0.970	0.970	0·960
100	0.968	0 964	0·950	0.948	0.944	0·938
120	0·946	0·941	0·931	0·912	0·912	0·914
140	0.912	0·911	0·900	0·976	0.889	0.881
160	0·888	0.881	0·874	0·860	0·859	0·852
180	0·871	0·871	0·863	0·852	0·040	0·852
200	0·886	0·889	0·873	0·069	0 858	0·862
220	0·906	0.906	0·893	0·882	0·880	0·884
240	0·929	0.927	0·914	0·910	0·901	0·909
260	0·916	0·948	0.932	0·931	0·922	0·926
280	0·951	0·954	0·945	0·910	0.999	0·933
300	0·951	0·947	0.915	0.994	0.994	0·998
320	0.942	0·958	0·941	0.926	0.026	0·927
340	0.942	0·938	0·987	0.991	0·923	0.929
360	0.919	0·950	0·940	0.942	0·994	0·919
380	0.961	0·905	0.959	0·956	0.951	0.0'4
400	0.979	0.978	0·97·1	0·971	0·969	0··69
420	0·989	0·988	0.986	0.004	0.985	0·.83
440	0·998	0·993	0·995	0·991	0.993	0.9.3
460	1.000	0.998	0.998	0·999	0·998	0·999
480		1·000	1.000	1.000	1·000	1·000
			5199·327Å* C_5			
0	0.981	0·964	0·965	0·963	0.964	0·963
20	0.964	0·964	0.964·	0·963	0.968	0·960
40	0·961	0·961	0·956	0.959	0·058	0·950
60	0·956	0·957	0.948	0.948	0·038	0·937
80	0.930	0.944	0.922	0.926	0·908	0.910
100	0.910	0·907	0·890	0·894	0.882	0·882
120	0.881	0·872	0·869	0·868	0.855	0.851
140	0·864	0.861	0·863	0·859	0.848	0·841
160	0·877	0·071	0·872	0.862	0.854	0·852
180	0·900	0·895	0.888	0·879	0·874	0·876
200	0.920	0·912	0·908	0·899	0·895	0·892
220	0.928	0·920	0·914	0·910	0.900	0·900
240	0·921	0·916	0·910·	0.904	0 898·	0.891
260	0.902	0·908	0·903	0.894	0.890	0.881
280	0·910	0.902·	0.898	0.892	0.889·	0.886
300	0·928·	0·908	0.906·	0·904	0.900	0.898
320	0.949	0·030·	0·923	0·918	0.914·	0.911
340	0.931	0·048·	0.939	0.939.	0.945·	0.950
360	0·955·	0·054·	0·946·	0·941·	0·997·	0.948
380		0.954·	0·948·	0·917	0.943	0·942

*Indicates that residual intensities have been measured from this position, in steps of 20mÅ towards the long wavelength region.

THEORETICAL LINE PROFILES

Calculation of line profiles requires that $I_c(\lambda,\mu)$ the continuum intensity and $I_l(\lambda,\mu)$ the line intensity be computed. These calculations have been based on the assumption that:

1. Local thermodynamic equilibrium conditions are valid in this problem.
2. Lines are formed by pure absorption.
3. Molecular lines are not affected by damping, so that only pure Doppler profiles are calculated.

Continuum Intensity

In choosing the model atmosphere two factors were considered. Firstly that the carbon constituent molecules are formed in the transition region between the photosphere and the chromosphere and all three molecules under study have been observed in emission. Therefore, the model atmosphere covering very small values of optical depth is required. Secondly the ability of standard photospheric models to explain observations of CO and MgH molecules indicate that cold models with T≒3900° K advocated by Pecker (1957) are probably ruled out. Also an analytical model based on observations is more suitable. Therefore, from $\log \tau_o = -1.6$ to $\log \tau_o = +0.6$ Pierce—Waddell (1961) model was used. This model was extended beyond $\log \tau_o = -1.6$ by combining it with the model given for the lower Chromosphere by Thomas and Athay (1961). This extends upto $\log \tau_o = -5.0$. Table III gives the adopted model. The last column gives the total absorption coefficient K_λ per atom of neutral Hydrogen in the continuum.

TABLE III

Pierce - Waddell HAO Model

$\log\tau_o$	T in degrees K	P_g in $\times 10^4$ dynes/cm	P_e in 10^4 dynes/cm	K in μ - ^{24} per neutral hydrogen atom
−5.0	6150	0.0071	0.0010	0.1402
−4.8	6060	0.0089	0·0030	0.1937
−4.6	5940	0·0123	0·0038	0·1616
−4.4	5820	0.0182	0.0038	0.1759
−4.2	5675	0.0275	0.0039	0 1984
−4.0	5585	0.0427	0.0038	0.2064
−3.8	5490	0.0646	0.0036	0.2106
−3.6	5390	0.0977	0.0035	0.2200
−3.4	5280	0.1413	0.0037	0.2593
−3.2	5140	0.2130	0.0040	0·2988
−3.0	5050	0.3107	0.0045	0.3642
−2.8	4955	0.4365	0·0054	0.4700
−2.6	4870	0.5957	0.0062	0.5803
−2.4	4790	0.7943	0.0072	0.7316
−2.2	4720	1.0720	0.0087	0·9407
−2.0	4680	1.4130	0.0109	1.2119
−1.8	4690	1.8520	0.0132	1.4805
−1.6	4740	2.3990	0.0164	1.7991
−1.4	4842	2.9240	0.0211	2.0457
−1.2	4976	3.7760	0.0288	2.4891
−1.0	5141	4.8870	0.0404	3.0148
−0.8	5339	6.3100	0.0598	3.7945
−0.6	5575	8.0540	0.0944	5.1547
−0.4	5805	10·0000	0.1660	7.0028
−0.2	6130	11.9000	0·3206	12.0860
−0.0	6469	13.9900	0.6622	20·5280
+0·2	6898	15.6700	1.4060	36.2100
+0.4	7362	17.2200	3.5240	76.9500
+0.6	8005	18·4500	9.3760	191.2600

$$K_\lambda = R_\lambda\ (H^-).Pe + K_\lambda\ (H) \qquad (1)$$

$K_\lambda\ (H^-)$ were taken from Gingerich (1960)

$K_\lambda\ (H^-)$ and $K_\lambda\ (H)$ are the absorption coefficients due to H_λ and H respectively and Pe the electron pressure.

$$K_\lambda(H) = \frac{C}{\nu^3}\left(1 - e^{-\frac{h\nu}{kT}}\right) e^{-\frac{\chi}{kT}} \sum_{n=3}^{9} \frac{e^{\frac{\chi}{n^2 kT}}}{n^3} + \frac{e^{\frac{\chi}{81kT}}}{2\chi kT}$$

is evaluated for every level of the model.

The emergent intensity in the continuum is given by (2)

$$I_0(\lambda,\mu) = \int_0^\infty S_\lambda\, e^{-\frac{\tau_\lambda}{\mu}}\, d\tau_\lambda/\mu \qquad (3)$$

where S_λ is the source function

Replacing S_λ by B_λ the Planck function,

$$I_c(\lambda,\mu) = \int_0^\infty B_\lambda\, e^{-\frac{\tau_\lambda}{\mu}}\, d\tau_\lambda/\mu \qquad (4)$$

$$\text{with} \quad d\tau_\lambda = \frac{K_\lambda}{K_0} d\tau_0 \quad , \quad \tau_\lambda = \int_0^{\tau_0} \frac{K_\lambda}{K_0}\, d\tau_0 \ ;$$

τ_0 being the optical depth at $\lambda = 5000°A$

$$I_c(\lambda,\mu) = \int_0^\infty B_\lambda\, e^{-\frac{\tau_\lambda}{\mu}}\, \frac{K_\lambda}{K_0}\, \frac{d\tau_0}{\mu} \qquad (5)$$

The integration is performed over log τ_0 rather than τ_0. Numerical integration was performed using Gregory's formula upto the first difference. It is seen from the expression for $\tau\lambda$ that to obtain $\tau\lambda$ at any level, it is necessary to integrate over all overlying layers. $\tau\lambda$'s have, therefore, been calculated only for log $\tau_0 = -4.2$ and downwards.

Table IV gives the continuum intensities so calculated.

TABLE IV

Continuum Intensities, $I_c(\lambda) \times 10^{-5}$

Wavelength	$\mu=1.00$	$\mu=0.80$	$\mu=0.60$	$\mu=0.45$	$\mu=0.35$	$\mu=0.25$
3660A°	2.037	1.861	1.599	1·340	1·130	0.915
4220A°	2.403	2.188	1.892	1.603	1.381	0.134
5000A°	3 059	2.799	2.436	2.115	1.869	1.593

Line Intensity

The emergent intensity in the line is given by

$$I_\ell(\lambda,\mu) = \int_0^\infty B_\lambda \, e^{-\frac{t_\lambda}{\mu}} \, dt_\lambda / \mu \qquad (6)$$

t_λ the line optical depth is defined by

$$dt_\lambda = (1+\eta_\lambda)\, d\tau_\lambda \qquad \eta_\lambda = \alpha_{\Delta\lambda} / K_\lambda \qquad (7)$$

$\alpha\Delta\lambda$ the line absorption coefficient at a distance $\Delta\lambda$ from the line centre λ_o is expressed in terms of the Doppler width $\Delta\lambda_D$ as

$$\alpha_{\Delta\lambda} = \frac{\sqrt{\pi}\, e^2}{m c^2} \int \lambda_o^2 \, \frac{N_{AB}}{\Delta\lambda_D} \exp\left(-\frac{\Delta\lambda^2}{\Delta\lambda_D^2}\right), \quad \frac{\Delta\lambda_D}{\lambda} = \frac{\xi}{C} \quad \text{and} \quad \xi^2 = \frac{2RT}{M} + \xi_t^2 \qquad (8)$$

ξ_t being the line of sight turbulence velocity; other symbols have their conventional meaning. The assumption of a Maxwellian distribution for turbulence is one of convention. Further this seems reasonable in so far as it provides a numerical estimate of turbulence velocity, for eddy sizes of the order of L; here L is the length of the line forming region.

f values adopted for CN, C_2 and CH were .026, .024 and .005 respectively. For CH the arbitrarily low value of .005 had to be chosen following Pecker and Praderie (1960) because with $f_{CH} = .06$ (de Jager and Neven 1957) the absorption coefficients obtained were high by a factor of 100.

The fraction of molecules capable of absorbing the frequency corresponding to the line of interest, N_{AB}

$$N_{AB} = i \times p(AB) \quad \frac{(2J+1)}{Z(AB)} \quad \exp(-B_J\, J(J+1)\, hc/kT \qquad (9)$$

where

p (AB) — Partial pressure of AB $= \dfrac{p(A) \times p(B)}{K_{(AB)}}$

Z (AB) — Partition function

i — Strength factor depends on the coupling scheme

B_J — rotational constant

TABLE V

Relative Partial Pressures—CN, CH and C_2

Log τ_0	P_{CN}/p_g	P_{CH}/p_g	P_{C_2}/p_g
−5.0	938.9E−11	106·0E−12	162.1E−14
−4.8	590.7E−14	170.2E−12	245.6E−14
−4.6	915.5E−14	266.5E−12	137.7E−14
−4.4	226.2E−13	481 8E−12	844.8E−14
−4.2	513.7E−13	888.1E−12	178·0E 13
−4·0	102.4E−12	157.7E−12	311·2E−13
−3 8	206.4E−12	273.1E−11	660·1E- 13
−3.6	140.3E−12	480.7E−11	182.7E−12
−3.4	109.3E−11	900.8E−11	288 2E -12
−3·2	212.0E−11	158.2E−10	562.7E−12
−3.0	420.6E−11	279.0E−10	108.3E−11
−2.8	036.7E−11	446.1E−10	189.4E−11
−2.6	156.9E−10	711.4E−10	355.0E 11
−2·4	284.5E−10	110.2E−09	611.9E 11
−2.2	505.6E−10	170.0E−09	103.7E -10
−2·0	778.6E−10	241.7E−09	155.5E- 10
−1.8	079.2E−10	311.1E−09	196.8E - 10
−1·6	102.9E−09	362.9E−09	214.0E−10
−1.4	844.5E−10	364.7E−09	107.6E−10
−1.2	661.8E−10	366.8E−09	159.6E−10
−1·0	478.9E−10	359.2E−09	127.1E−11
−0.8	321.9E−10	336.7E−09	990.5E−11
−0·6	109·9E−10	301.8E−09	663.7E -11
−0.4	129.9E−10	272.6E−09	479.2E- 11
−0.2	676.9E−11	216.7E 09	285.6E−11
0.0	359.5E−11	171.1E−09	172.2E −12
0·2	180.9E−11	129.2E− 09	986.9E -12
0.4	793.3E−12	901·1E−10	701.9E−10
0.6	309.4E−12	584.7E−10	230.9E 12

Table V gives the partial pressures calculated by solving simultaneously the equations,

$$P(H) = p(H)\,[(1+2\,p(H)]\,/\,K(H_2)\,) \tag{10}$$

$$P(C) = p(C)\,[(1+p(H)]/K(CH)+p(O)/K(CO)\,) \tag{11}$$

$$P(N) = p(N)\,[(1+2p(N)]/K(N_2)+p(H)/K(NH) \tag{12}$$

$$P(O) = p(O)\,[(1+p(C)]/K(CO)+p(H)/K(OH) \tag{13}$$

and

$$K_{AB} = g_A\, g_B \left(\frac{2\pi m k T}{h^2}\right)^{\frac{3}{2}} \frac{h^2}{8\pi^2 I}\left(1 - e^{\frac{\omega hc}{kT}}\right) e^{-\frac{D_0}{kT}} \tag{14}$$

where fictitious pressures P (H), P (N), P (C) and P (O) are derived from a system of assumed abundances (Goldberg, Muller and Aller 1960) of these elements. The dissociation potentials D_0 were taken from P.G. Wilkinson (1964).

$$\alpha_{\Delta\lambda} = \frac{\sqrt{\pi}e^2}{mc^2} f \frac{\lambda_0^2}{\Delta\lambda_D} \frac{p_{(AB)}}{p_{(H)}} \frac{1}{Z_{(AB)}} \exp(-B_y J\overline{J+1} \frac{hc}{kT}) e^{-\left(\frac{\Delta\lambda}{\Delta\lambda_D}\right)^2} \qquad (15)$$

Turbulence

Since the effective layer of molecular line formation is narrower than that of atomic lines, a depth independent anisotropic model was chosen.

$$\xi_t^2 = \xi_{tan}^2 - \mu^2(\xi_{tan}^2 - \xi_{rad}^2) \quad ; \quad \Delta\lambda_D^2 = \frac{\lambda_0^2}{c^2}(\frac{2RT}{M} + \xi_t^2) \qquad (16)$$

ξ_{rad} is obtained by fitting the observed and calculated profile at $\mu = 1.0$ while ξ_{tan} was fixed by a fit at $\mu = 0.25$.

The calculation of line contours for doublets or triplets were essentially the same, except that for each level the absorption coefficients of constituent lines were added, with the appropriate wavelength shift. If $\Delta\lambda_s$ is the separation in wavelength between two lines at λ_1 and λ_2 then the total absorption coefficient $\alpha_{\Delta\lambda}$ at $\Delta\lambda$ from λ_1 is given by

$$\alpha_{\Delta\lambda} = \alpha_1 \exp[-(\Delta\lambda/\Delta\lambda_D)^2] + \alpha_2 \exp[-(\Delta\lambda \mp \Delta\lambda_s)^2 / \Delta\lambda_D^2] \qquad (17)$$

α_1 and α_2 are the absorption coefficients at the two line centres. This involves no approximation; in all cases of molecular blending, the two lines have very close initial and final energy states. So the blending lines have identical conditions of excitation and the total line absorption coefficient at any wavelength is the sum of all the absorption coefficients at that wavelength

$$\alpha_{\Delta\lambda} = \sum_i \alpha_{\Delta\lambda_i}$$

It is important to note that $\Delta\lambda_i$ is not measured from the central wavelength of the blend, but from the centre of one of the constituent lines. With an IBM 1620 Computer calculation of a single residual intensity took 225 seconds for a singlet and 290 seconds for a doublet.

Calculations and Comparison with observations

Trends in observed centre—limb variations emphasise that these variations are very similar for strong lines on the one hand and weak lines on the other, irrespective of the molecule of their origin. So computations were performed for a restricted set of lines, so that characteristic features of the observed variations could be studied. The CN lines of 3864A, and 4207A, C_2 lines of 5094A and 5147A and CH lines of 4210A and 4281A were selected for extensive computation.

Each of these lines is a spin doublet except 5094.029A of C_2 which is a triplet. The hyperfine structure of atomic lines widens the line considerably and simulates the effect of turbulence. Therefore, fine structure due to spin doubling has to be properly accounted for in order to arrive at the correct values for ξ_t

The construction of an unresolved doublet profile to which the correct turbulent velocity must be fitted is complicated. The contour is very sensitive to the separation between the lines and a very small change in this separation changes the profile considerably. Preliminary calculations also indicated that the use of the rigorous doublet approach is necessary for separations larger than about 25mA. Also the relative intensities of the two component lines is very important in reproducing exactly the asymmetries observed and the location of the central wavelength.

Published data on separations for spin doubling are probably accurate upto 10mA corresponding to 0.75 km/sec at 4000A. Also the smallest resolvable separation in wavelength is 15mA. Therefore, a spin doublet of separation of 15mA or less may be treated as a coincident doublet with the absorption coefficients of the two lines added, without any wavelength shift.

The 3864.307Å line of CN has a spin separation of less than 15mA., ξ_{rad} was first calculated by choosing the appropriate numerical fitting factor F, to match the observed central intensity. F would generally give a measures of the uncertainties in the transition probabilities. The value of ξ_{rad} was then adjusted to give the best fit for the entire profile. The adjusted value of $\xi_{rad} =$ 3 km/sec.

With this ξ_{rad} and F, the observed half width at $\mu = 0.25$ was matched by adjusting ξ_{turb}. A good overall fit was difficult to obtain, because if the half width were exactly matched the central intensities were too low. ξ_{turb} giving the correct central intensity at $\mu=0.25$ was improbably large and gave very broad profiles. In order to fix ξ_{turb} therefore, the observed C-L variations of the profile over the disc, had to be considered. The optimum value of ξ_{turb} giving the observed trends was 3.6 km/sec (Fig.3). When the numerical fitting factor F was changed to fit the central intensity at every μ and $\xi_{rad} =3$ km/sec and $\xi_{turb} =3.6$ km/sec were used in computing profiles, the theoretical profiles matched the observed ones remarkably well. A plot of $F\mu$ versus μ is a straight line with $F_{1.00} \simeq \frac{1}{3} F_{0.25}$ This is a surprising result in as much as F was expected to characterise uncertainties in physical constants. This also indicates that a change in the assumed turbulence velocity field will not improve the agreement significantly and in fact the values derived for ξ_{turb} and ξ_{rad} above are certainly the appropriate ones.

4207.409 of CN and 5094.029Å of C_2 were chosen for detailed multiplet calculations as these seemed to have the most reliable separations available in literature. For the first line, wavelengths of the constituent lines were measured by Heurlinger (1918)*.

Detailed calculations showed that this separation of of 69mA could not reproduce the observed profile exactly, for any value of ξ_{rad} at the centre of the disc. Further calculations showed that with this separation, the best overall match was obtained with $\xi_{rad} =3$ km/sec. So, to improve the agreement, the only other alternative was to change the value of the separation. For $\Delta\lambda_s = 60$mA the fit at the centre of the disc is very good. That a decrese of 10mA in $\Delta\lambda_s$ improves the fit to such a large extent, emphasizes the need for knowing these separations very accurately.

As in the case of 3864.307Å of CN the fit at $\mu = 0.35$ could not be made exactly and $\xi_{turb} = 3.6$ km/sec provided the best over-all agreement from centre to limb.

The 5094.029Å line of C_2 consists of a triplet of the P branch J = 62. P_2 (62) and P_3 (62) are coincident for all practical purposes and P_1 (62) is 93 mA away at 5094.095Å

* I am indebted to Mrs. Moore-Sitterly for loaning a copy of Heurlinger's results from his Lund thesis.

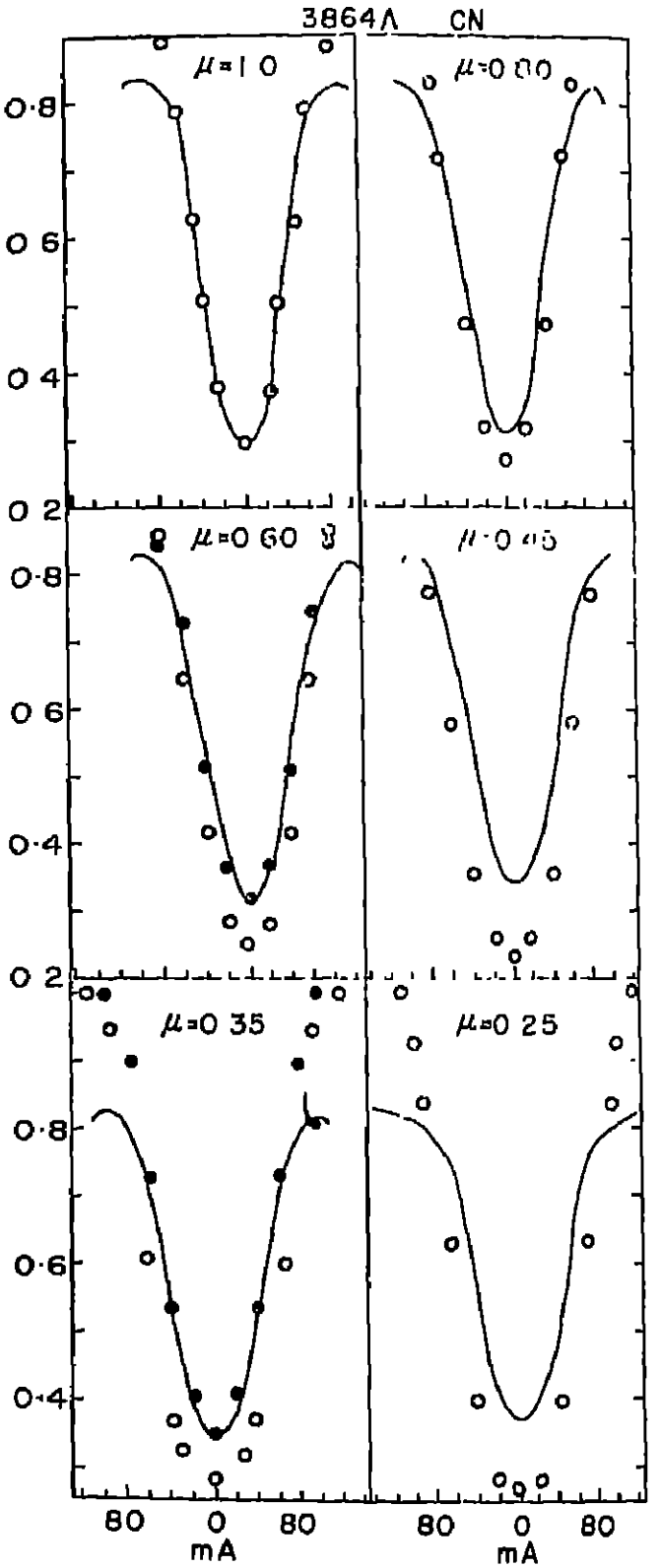

Fig. 3. Observed and calculated profiles. ξ_{rad} and ξ_{tan} are 3.0 km/sec. and 3.6 km/sec respectively. Observed-continuous line; calculated-open circles. At $\mu=0.60$ and 0.35, filled circles give the calculated profile with different fitting factors.

Fig. 4a gives the computed and observed profiles, for the two lines, at three disc positions.

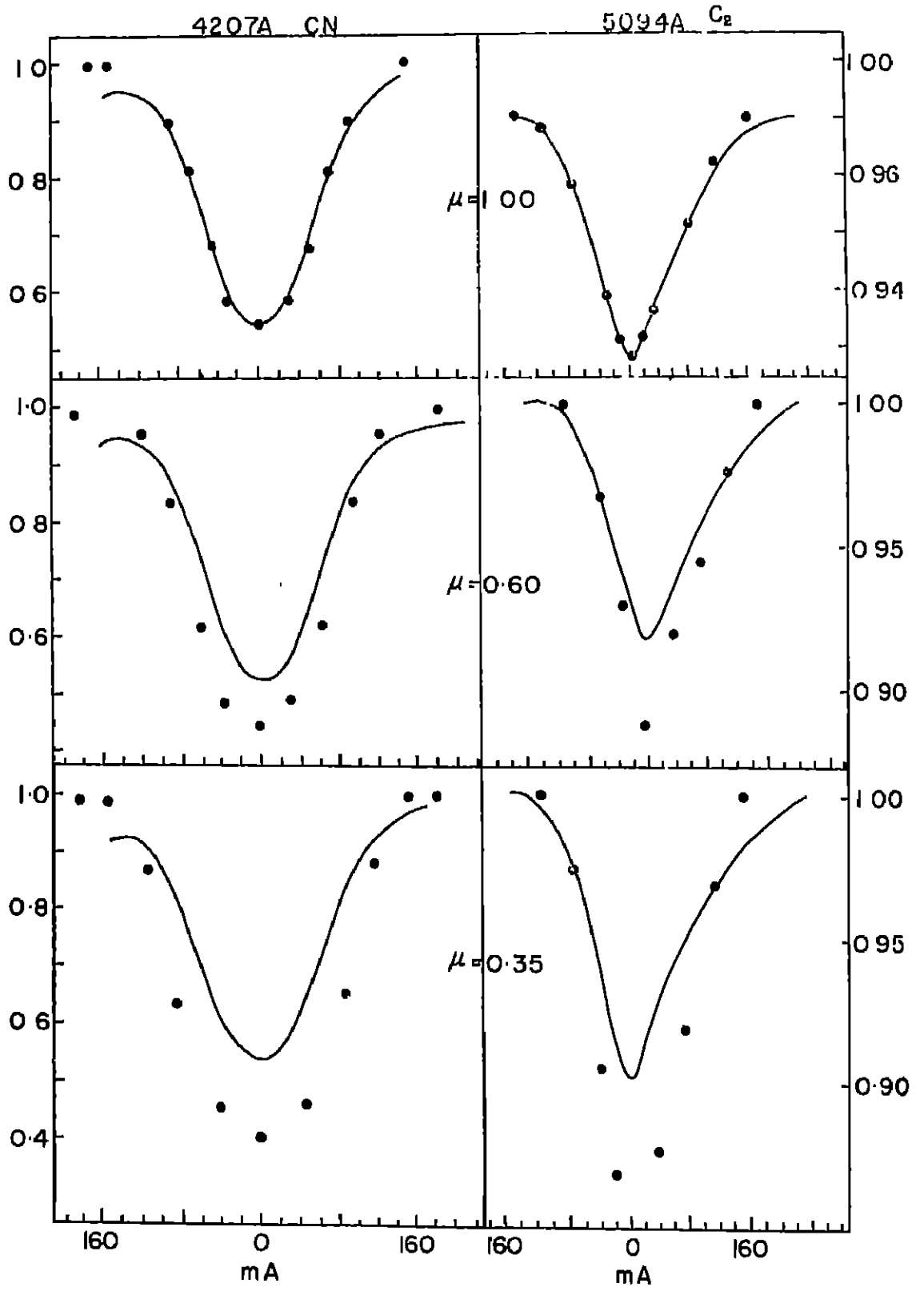

Fig. 4(a). Observed and calculated profiles on the doublet assumption.

Detailed calculations of doublets showed that:

(1) the half width and shape of a profile is fixed by a unique combination of $\Delta\lambda_r$, ξ_{rad} and ξ_{tan}

(2) the actual value of $\Delta\lambda_r$ is very critical in exactly reproducing the observed profile, if $\Delta\lambda_r$ is the same order of magnitute as $\Delta\lambda_D \leftrightarrows 50$mA.

(3) $\Delta\lambda_r \lesssim$ 20mA leads to a situation where turbulence broadening dominates and the line may be treated as single.

(4) For $\Delta\lambda_r >$ 80mA, doublet calculations correctly reproduce, the asymmetries in the wing and the half widths are not affected.

Considering the fact that spin separations are so ill known, time consuming doublet calculations on a medium speed computer were not justified. The rest of the selected profile were calculated as singlets. As a tie-in with the doublet calculations, ξ_{tan} and ξ_{rad} were re-determined for 4207 Å CN and 5094 Å C_2, treating them as single lines. $\xi_{rad}=4$ km/sec and $\xi_{tan}=5$ km/sec were obtained for the best fits. This incidentally shows that the ratio of ξ_{tan}/ξ_{rad} has remained more or less the same in both cases giving an anisotropy factor of 1.2. This is an indication of the reality of the existence of anisotropy in the transition region between the photosphere and the chromosphere.

The same set of turbulence velocities were used in obtaining fits for the lines 4210A of CH, 4281A CH, and 5147A of C_2. The results are given in Fig. 4b, Fig. 5a, and Fig. 5b.

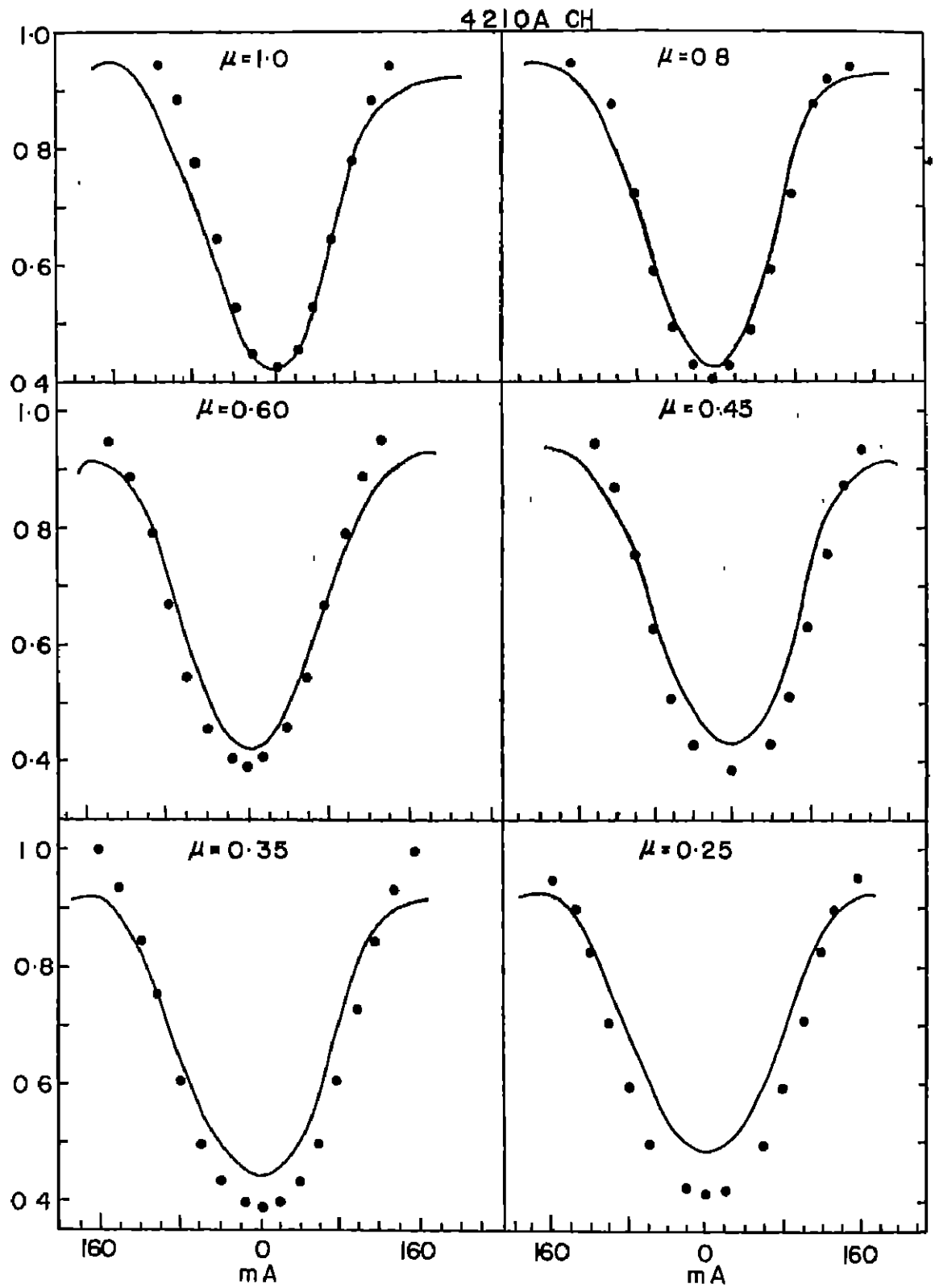

Fig. 4(b). Observed and calculated profile on the singlet assumption.

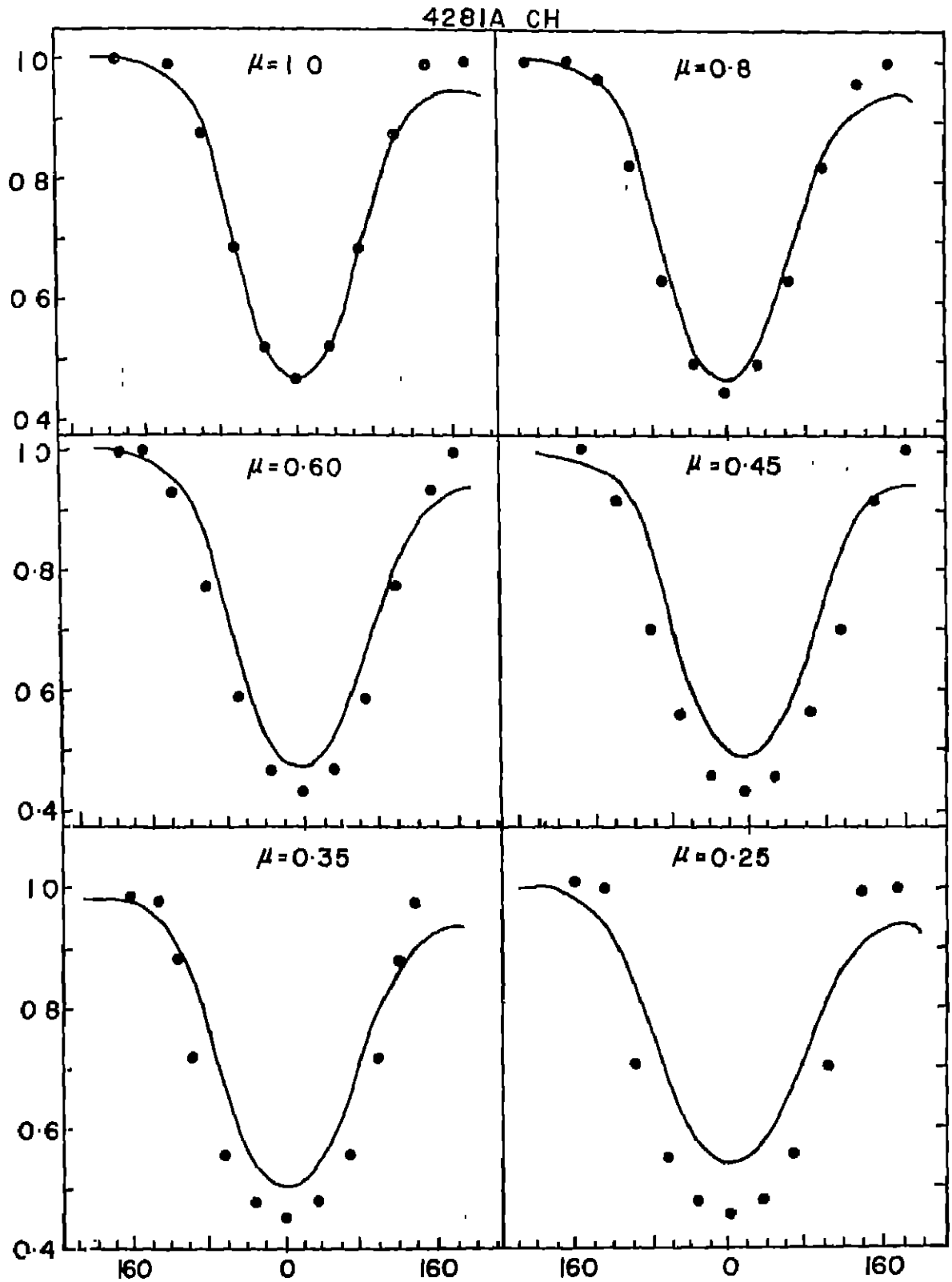

Fgl. 5(a). Calculated and observed profiles on the singlet assumption.

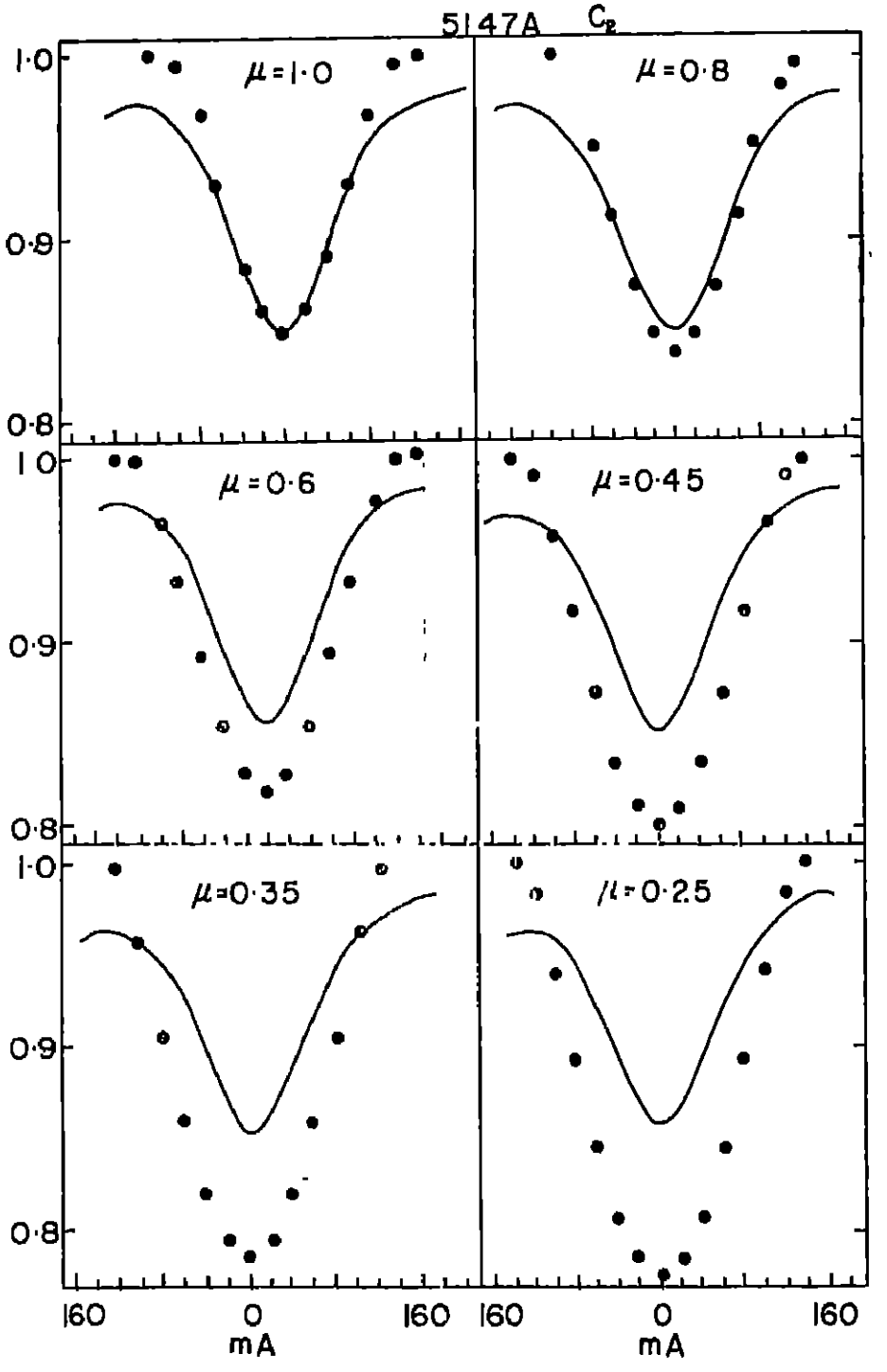

Fig. 8(b). Calculated and observed profiles on the singlet assumption.

The computed profiles for positions other than the centre are broader and deeper than observed ones. Although the trends of C-L variation of central intensities are similar, they are by no means identical (Fig. 6).

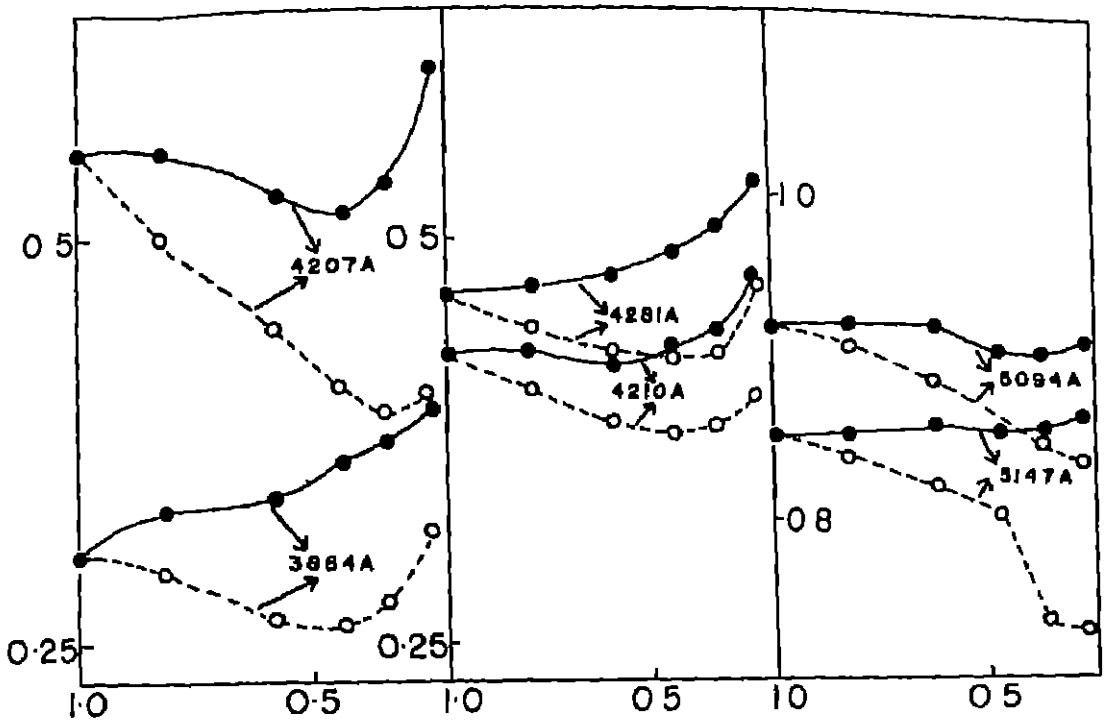

Fig. 6. Variation of central intensities with μ observed—continuous curve; calculated-dashed curve.

Once again if F was changed to fit the central intensity at each μ position, the combination of ξ_{mic}=5.1 km/sec and ξ_{mac}=4.0 km/sec gives strikingly good profile fits. Th normalised variation of $F\mu$ versus μ has been plotted for each line in Fig. 7.

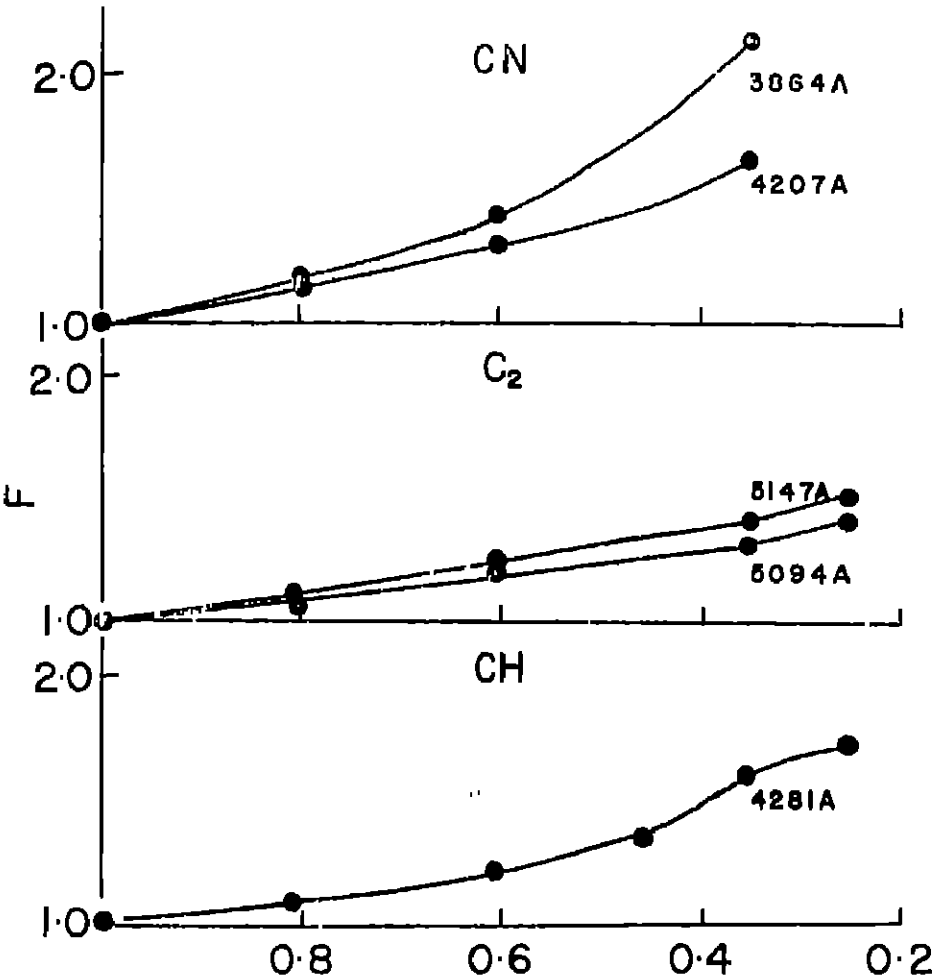

Fig. 7. Variation of normalised "fluing factors" from centre to limb.

DISCUSSION

The results presented so far draw attention to three facts. First of all the calculations for lines 3864Å CN, 4207Å CN and 5094Å C_2 establish that $\xi_{rad}=3$ km/sec. The value 3.6 km/sec for ξ_{tan} is less certain, although it represents the C-L variation of the profiles best.

The second result of interest is that, calculations based on the singlet assumption lead to higher values for ξ_t; but the same value of 4 km/sec and 5.1 km/sec for ξ_{rad} and ξ_{tan} seems to fit all the observations uniformly well, in spite of the fact that the separations (which are not known) are certainly not the same. In order to understand this result, it is necessary to recall that although the value of $\Delta\lambda_t$ is very critical in achieving an exact fit with the observed profile, for any given $\Delta\lambda_t \pm 15$ mÅ of the true $\Delta\lambda_t$, one unique value of ξ_t gives the best over-all fit. This is borne out by the fact that both 4207Å CN ($\Delta\lambda_t = 60$mÅ) and 5094Å C_2 ($\Delta\lambda_t = 93$mÅ) give best fits for $\xi_{rad}=4.0$ km/sec and $\xi_{tan} = 5.1$ km/sec. It must however be pointed out that these conclusions are strictly valid for doublet lines whose intensities are almost the same, as is true for molecular spin doublets of high J. These conclusions are not valid for atomic hyperfine structure where there is a wide range of intensities for the component lines.

The fact that a change in F for different μ positions results in reproducing the observed profile almost exactly is striking. Of course changing F with μ removes the one physical restriction imposed on comparing a set of theoretical profiles with the observed profile. But in fitting profile shapes rather than equivalent widths, changing F with μ, does not make the matching calculations entirely arbitrary. On the other hand such a systematic variation of F with μ may very well have some physical significance.

The only plausible factor that could cause the variation in F, must arise from variations in partial pressures of the molecules. Since all three molecules are similarly affected, the amount of free carbon available for the formation of C_2, CN and CH must be a parameter affecting the C-L observations. This leads us to question the assumption that $T_{Excitation} \simeq$ Tc. Newkirk (1957) has reached the interesting conclusion that de Jager's (1952) model with hyper dissociation Td $\neq$ Tc explains the C-L variation of CO lines as well as do the Aller-Pierce or the Minnaert models. The explanation of the CO observations on the basis of Td $\neq$ Tc is important in as much as a similar treatment of C_2, CN and CH might provide a unified explanation for all the four molecules. CO with its high dissociation potential and high concentration at the very highest layers of the Sun is capable of depleting the free carbon supply considerably and, therefore, affect the partial pressures of the other carbon constituent molecules very significantly. The variation of F μ has most probably a bearing on this question.

SUMMARY AND CONCLUSIONS

By carrying out detailed line profile calculations for selected molecular lines of CN, CH and C_2 on the basis of LTE and an anisotropic model of turbulence the radial turbulence velocity is established to be 3.0 km/sec. A tangential turbulence velocity of 3.6 km/sec provides the best description of the C-L variation of the profiles. These values pertain to the region $\tau_o = .04$ to $\tau_o = 0.1$ of the solar atmosphere.

It has been shown that if the separation due to spin doubling is neglected the velocities derived are too high. This increase, however, is independent of the separation $\Delta\lambda_t$ as long as the two blending lines are of comparable intensity and $\Delta\lambda_t$ is of the order of $\Delta\lambda_D$, the doppler width. Singlet calculations of ξ_{rad} and ξ_{tan} based on this conclusion provide additional confirmation in the values 3.0 km/sec and 3.6 km/sec respectively.

A very interesting variation of the fitting factor F with μ is observed. There is striking similarity of these variations from line to line. Although no quantitative confirmation is available, it is suggested that the explanation of this variation ought to be associated with the inequality $T_{dissociation} \neq T_{electron}$.

Excellent matching obtained at the centre of the disc between observed and computed profiles prove that the assumption $S_\lambda = B_\lambda$ for the molecular carbon lines is certainly adequate, a fact that is also borne out by consistent values of $T_{rotational}$ obtained for these molecules. Regarding the treatment of dissociation equilibrium, however, the implicit assumption of LTE is questionable. Further work is planned for examining this question quantitatively. It is hoped that this would throw further light in explaining the C-L observations of the carbon molecules.

It is a pleasure to thank Dr. M. K. V. Bappu for his constant interest and encouragement. Extensive help rendered on many aspects of the problem by Dr. A. Bhatnagar is gratefully acknowledged. The research was carried out during the tenure of a Senior Research Scholarship of the Ministry of Education, Government of India, tenable at the Kodaikanal Observatory.

KODAIKANAL OBSERVATORY;
September, 1968

REFERENCES

Bracewell, R.N., 1955, J. Opt. Soc. Am. **45**, 873.
Cowley, C.R., 1964, Astrophys. J., **139**, 731.
Gingerich, O.J., 1961, Thesis, Harvard University.
Goldberg, L., Aller, L.H. and Miiller, E.A. , 1959, Astrophs. J. Suppl. **5**, 1.
Heurlinger, 1918, Lund Thesis.
Jager C.de., 1952, Rech. Astr. Obs. Utrecht. Vol. **13**, Part I.
Jager, C. de., and Neven, L., 1957, Mem. Soc. Roy. Sc. Liege, **18**, 357.
Laborde, G., 1961, Ann. Astrophys., **24**, 89.
Newkirk, G. A., 1957, Astophys. J., **125**, 571.
Pecker, J. C. and Peyturaux, R., 1948, Ann. Astrophys. **11**, 90.
Pecker, J. C., 1949, Ann. Astrophys., **12**, 9.
Pecker J. C., 1957, Mem. Soc. Roy Sc. Liege, **18**, 332.
Pecker, J. C., 1960, Ann. Astrophys., **23**, 622.
Pierce, A. K. and Waddell, J. H., 1961 Mem. R. astr. Soc., **68**, 89.
Thomas, R. N. and Athay, R. G., 1961, Physics of the solar Chromosphere, Inter Science Publishers, New York.
Waddell, J. H., 1962, Astrophys. J., **136**, 223.
Waddell, J. H., 1963, Astrophys, J., **137**, 1210.
White, O. R., 1961, Thesis, University of Colorado.
Wilkinson, P. G., 1963, Astrophys. J., **138**, 779.

MGIPCBE—88—9 DAOK/68 —9-10-69—375.

E R R A T A

KODAIKANAL OBSERVATORY BULLETIN NO. 187

Location	Error	Read.
Page A 149 First line of Abstract	Parts a Comet	Parts of a ormet